

CRYOGENIC RESONATOR COMPLEX

V. V. Parshin,^{1,2} * E. A. Serov,^{1,2} G. M. Bubnov,^{1,2}
V. F. Vdovin,^{1,2} M. A. Koshelev,¹ and
M. Yu. Tretyakov¹

UDC 537.86

We describe a unique new-generation laboratory facility for studying dielectric parameters of gases and condensed media, as well as reflectivity of surfaces (reflection loss) in the frequency range 100–500 GHz and pressure interval from 10^{-3} Torr to the atmospheric pressure at temperatures of 4 to 370 K. The Fabry–Perot resonators with Q-factors of about 10^6 , in which the studied gas, dielectric, or reflector are located, are the measuring elements of the facility. The backward-wave oscillator stabilized by the wideband phased-lock loop is the radiation source. Using this facility, we were able, in particular, to confirm the presence of water dimers in the atmosphere and study some materials for the reflectors of the “Millimetron” space observatory.

1. INTRODUCTION

Resonator (resonance-based) methods are widely used for high-precision measurements in all electromagnetic radiation frequency ranges, although each range has its peculiarities for developing resonance devices. In the millimeter- and submillimeter-wave ranges, variants of the classical open Fabry–Perot resonator with a Q-factor of up to 10^6 (in the case of reasonable geometric dimensions) are mainly used for studying gases and condensed media. Resonant frequencies and the resonance-curve linewidths of an empty resonator and a resonator with a sample are the measured values for calculating the refractive index n and the loss tangent $\tan \delta$ of solid and liquid dielectrics, metal-reflection losses, or the absorption coefficient in a gas. Frequency measurements have the maximum accuracy among all types of measurements, and the ultimate Q-factor for the resonators with uncooled mirrors (i.e., a large effective length of the path) ensures high sensitivity of equipment. The developed resonator facility is designed for obtaining precision frequency and temperature dependences of the studied-material parameters. The obtained information can be used for solving the following problems:

1. Studying the antenna reflectivity (including the antennas cooled to cryogenic temperatures) and the screens of ground-based/spaceborne radio telescopes with high-sensitivity superconducting receivers.
2. Studying reflectivity and determining reflection losses for high-quality mirrors of the power-transmission lines in the case of the highest power density at the mirrors manufactured from pure high-reflectivity metals (silver, copper, gold, and aluminum) and studying reflectivity of metals with impurities, alloys, and various coatings.
3. Study absorption in gases for developing precision models of electromagnetic-wave propagation in the Earth’s atmosphere and atmospheres of other planets.
4. Studying absorption in gas mixtures, including both resonant lines and nonresonant absorption, for the purposes of navigation, radar, and communication to recover vertical profiles of atmospheric temperature and humidity, etc.

* parsh@appl.sci-nnov.ru

¹ Institute of Applied Physics of the Russian Academy of Sciences; ² R. E. Alekseev Nizhny Novgorod State Technical University, Nizhny Novgorod, Russia. Translated from *Izvestiya Vysshikh Uchebnykh Zavedenii, Radiofizika*, Vol. 56, Nos. 8–9, pp. 614–621, August–September 2013. Original article submitted May 30, 2013; accepted September 30, 2013.

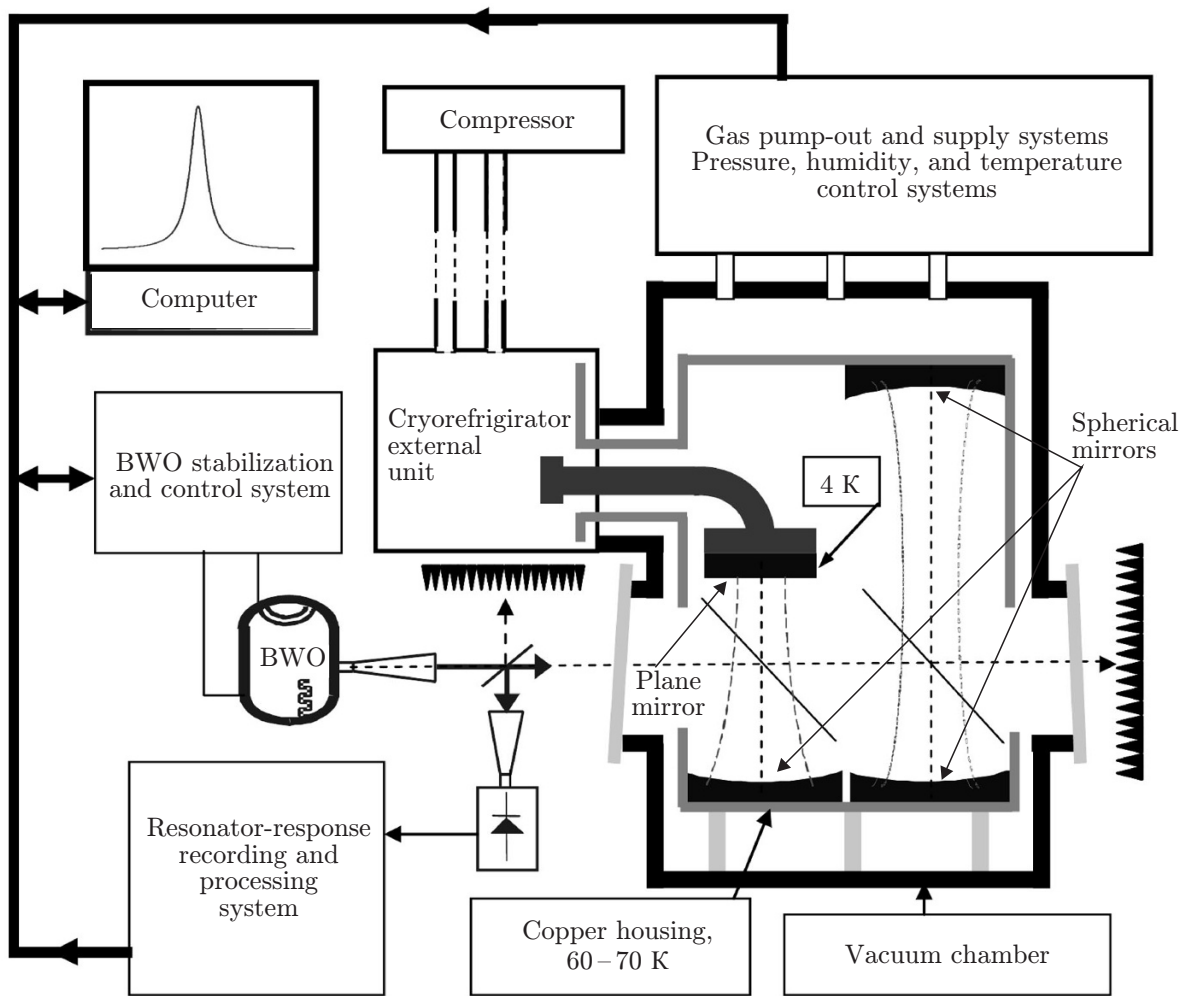


Fig. 1. Structural diagram of the facility.

2. EXPERIMENTAL FACILITY

The facility is based on the resonator spectrometer developed at the Institute of Applied Physics of the Russian Academy of Sciences [1–4]. The facility layout is shown in Fig. 1. The radiation loss in the material under study determines the Q-factors of two quasioptical Fabry–Perot resonators located in the vacuum chamber [5, 6]. The resonator lengths differ by a factor of two, i.e., the long (symmetric) resonator is formed by two identical spherical mirrors, whereas the short (nonsymmetric) resonator is formed by one spherical and one plane mirror. The systems of excitation, recording, and processing of the resonator signal are described in detail in [4–7]. By now, the resonator-spectrometer operating frequency range has been extended up to 520 GHz. To ensure operation in the range 350–520 GHz, a unit [8, 9] containing a backward-wave oscillator (BWO) and quasioptical and waveguide channels is employed. This unit has been constructed using the same principles as those for six units covering the range 36–360 GHz. The units can be interchanged within several minutes.

All the four resonator mirrors (three identical spherical mirrors and one plane mirror) in the gas-study facility have been manufactured by the same technology. The necessity of using two different-length resonators for measuring absorption in gases with water vapor is stipulated by the water-molecule adsorption on the mirrors and coupling elements of the resonator [6]. The measurement principle and the study results are presented in detail in [6, 9–12]. To equalize the in-chamber temperature, the resonators were placed in a copper housing with 5 mm-thick walls. The housing was equipped with copper tubes for a coolant, which

specified the operation temperature. The “Julabo FR 50” thermostating device was utilized to maintain the coolant temperature in the external loop with a stability of $\pm 0.01^\circ\text{C}$ in the temperature interval from -50°C to $+200^\circ\text{C}$. The chamber was equipped with a pressure- and temperature-control system and was thermally insulated from the surrounding medium. Measured gas injection and pumping were ensured by the vacuum system.

The results of studies of the water-vapor absorption spectrum using this experimental facility include the resolved rotational lines of the water dimers at room temperature, which were observed for the first time and published in [13].

In the facility for low-temperature studies of the mirror reflectivity, the symmetric resonator is used as a reference, whereas the studied reflector sample is mounted on a copper or aluminum mirror of the nonsymmetric resonator. To ensure thermal isolation from the resonator body, the mirror with the sample is fixed on fiberplastic supports and is coupled to the second cooling stage of the refrigerator by a flexible refrigerating line. The copper housing is coupled to the first cooling stage of the refrigerator and is also isolated from the chamber walls. Temperature gradient over the box does not exceed two degrees for 70 K. Before the cooling, the chamber cavity is evacuated to a pressure of 10^{-3} Torr by a “Pfeiffer Vacuum HiCube” turbomolecular pump.

The modified cryovacuum chamber [14] with “RDK-415D” closed-cycle cryocooler by Sumitomo Heavy Industries, Ltd with the Gifford–McMahon thermodynamic cycle of the helium-temperature level is used as the cryogenic basis of the facility. This refrigerator can ensure unloaded cooling to temperatures below 3 K and 60 K in the second and first cooling stages, respectively. With the actual load, such an efficiency is sufficient for reaching an equilibrium temperature of about 4 K of the sample, and about 70 K of the copper box after 48-h operation cycle.

The mirror, housing, and sample temperature is monitored by a “LakeShore Temperature Monitor” eight-channel automated system (Model 218) with the “Lake Shore DT-670B-CU” diode heat sensors with a certified accuracy of ± 0.5 K in the range 2–305 K.

The input/output windows of the radiation which excites the resonator are made of high-pressure polyethylene. This material has small losses in the millimeter- and submillimeter-wave ranges and ensures effective infrared-radiation filtering. The windows are mounted at an angle of about 10° to the output beam (see Fig. 1) to rule out that parasitic reflection of the radiation enters the receiving channel.

3. RESULTS OF THE STUDY OF REFLECTION LOSSES AT CRYOGENIC TEMPERATURES

The plane mirrors made of oxygen-free copper (with copper content 99.28 wt%), aluminum (with aluminum content 99.99 wt%), and a high-purity aluminum foil (the aluminum content exceeds 99.99 wt%) were studied in the range 100–200 GHz. The reflecting surfaces of the mirrors were treated by a diamond tool. The surface roughness is 10–20 nm.

A series of aluminum film reflectors for the radiothermal screens of the “Millimetron” space observatory [15] was also studied. Aluminum coating was applied to a 20 μm -thick polyimide film by the magnetron-sputtering method. The aluminum-layer thickness varied in the range 100–260 nm.

Energy losses due to reflection from metal samples for normal incidence were determined on the basis of the results of measurements of the resonator-response linewidth. The corresponding calculation method is described in detail in [16–18].

Since the measurements are impossible under the condition of a working cryocooler compressor because the sample vibration and, therefore, resonant response distortion, the sample was first cooled to a minimum temperature (about 4 K), the compressor was switched off, and the resonant-curve linewidths of the reference and measuring resonators during natural heating were recorded with the turbomolecular pump switched on.

Figure 2 shows the results of calculation of the reflection losses for four metals with maximum reflectivity for temperatures ranging from the room value to 4 K at a frequency of 150 GHz. Silver, which has the maximum reflectivity, was not considered because of its low corrosion resistance. The calculation

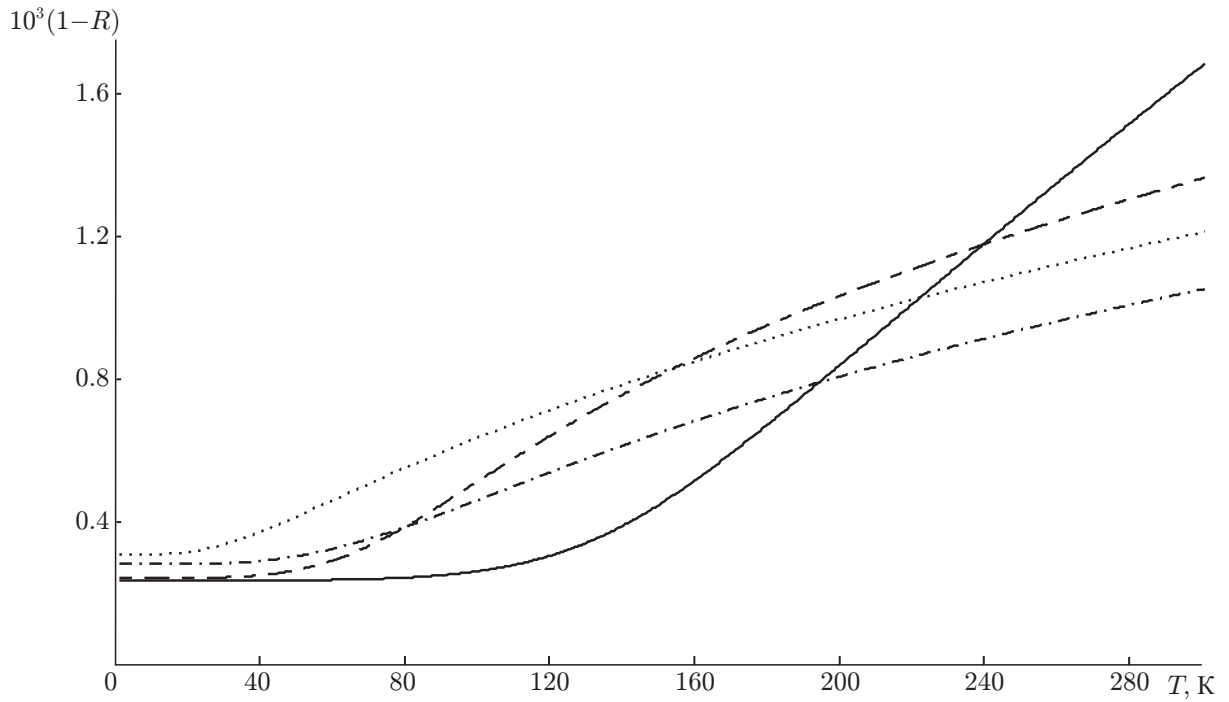


Fig. 2. Calculated temperature dependences of the loss (R is the reflection coefficient) during reflection from the most reflecting metals at a frequency of 150 GHz. The solid, dashed, dotted, and dash-dotted curves correspond to beryllium, aluminum, gold, and copper, respectively.

results are shown with allowance for the anomalous skin effect in the approximation of a spherical Fermi surface [19, 20]. It should be noted that beryllium (which has an anomalously high Debye temperature of 1481 K) is the most reflecting metal (see also [21]) for temperatures below 200 K to as low as liquid helium temperatures. These calculated dependences can be considered as the highest temperature dependences of reflection losses for metals with temperatures reaching the liquid helium values.

The reflection loss for a copper mirror made of oxygen-free copper (with copper content 99.28 wt%) was measured as a reference. The temperature dependence of the loss is shown in Fig. 3 along with the calculated loss for pure copper with allowance for the anomalous skin effect. It is seen that the loss exceeds the calculated value by about 20% and 100% for room temperature and the temperature below 40 K, respectively. The result is quite expected since the used copper sample contains admixtures which mainly determine the loss level at liquid helium temperatures.

Figure 4 shows temperature dependences of the reflection losses for aluminum samples and the calculation result for the loss in pure aluminum with allowance for the anomalous skin effect. Two aluminum mirrors (with aluminum content 99.99 wt%) produced by RusAl, which were similar to copper mirrors, and two mirrors of a high-purity aluminum foil (the aluminum content exceeded 99.99 wt%) were studied. It is obvious that the losses are close to calculated values for room temperatures, but differ by 10–15% for different samples and exceed the calculated values by approximately 80% at cryogenic temperatures. For high-purity aluminum, especially for the high-purity foil, such an increase in the loss is not quite clear. Nevertheless, the measurement results at temperatures above 80 K coincide with those previously obtained [17] in another resonator facility for other high-purity samples, where the losses were observed to increase compared with the calculated values at a temperature below 100 K.

Figure 5 shows the temperature dependences of the reflection losses for film reflectors of the “Milimetron” space observatory. Three film samples were studied. Sample 1 is an PM-1EU 20 μm -thick polyimide film covered by an aluminum layer (the aluminum content was 99.99 wt%) with a thickness of about 0.15–0.19 μm thick and a protective silicon-oxide layer of about 10–20 nm thick on the one side.

Samples 2 and 3 were made of the same polyimide film with one-sided aluminum coating (the

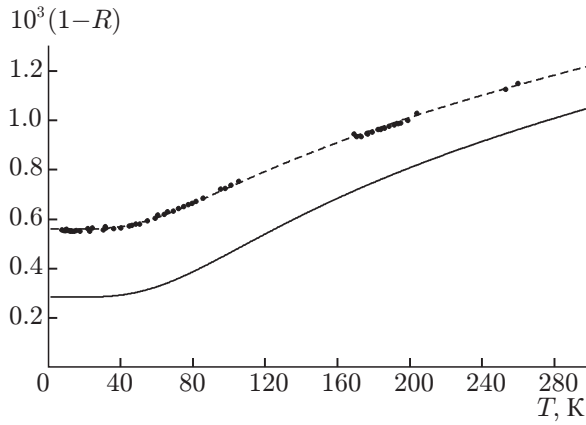


Fig. 3. Temperature dependence of the reflection loss (dots) and its approximation (dotted curve) for a copper mirror at a frequency of 150 GHz. The solid curve corresponds to the calculated reflection loss for pure copper with allowance for the anomalous skin effect.

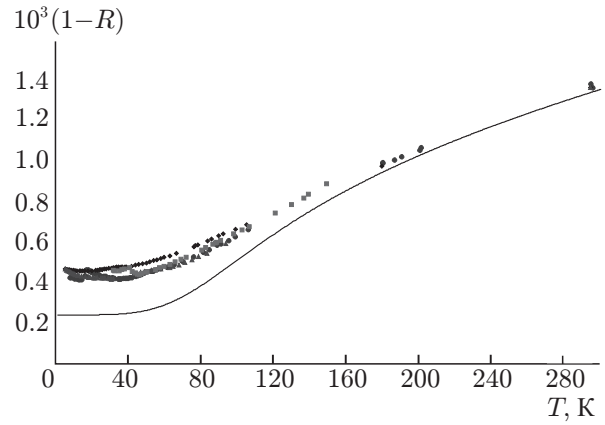


Fig. 4. Temperature dependence of the reflection loss for aluminum samples at a frequency of 150 GHz. The solid curve corresponds to the calculated reflection losses for pure aluminum with allowance for the anomalous skin effect.

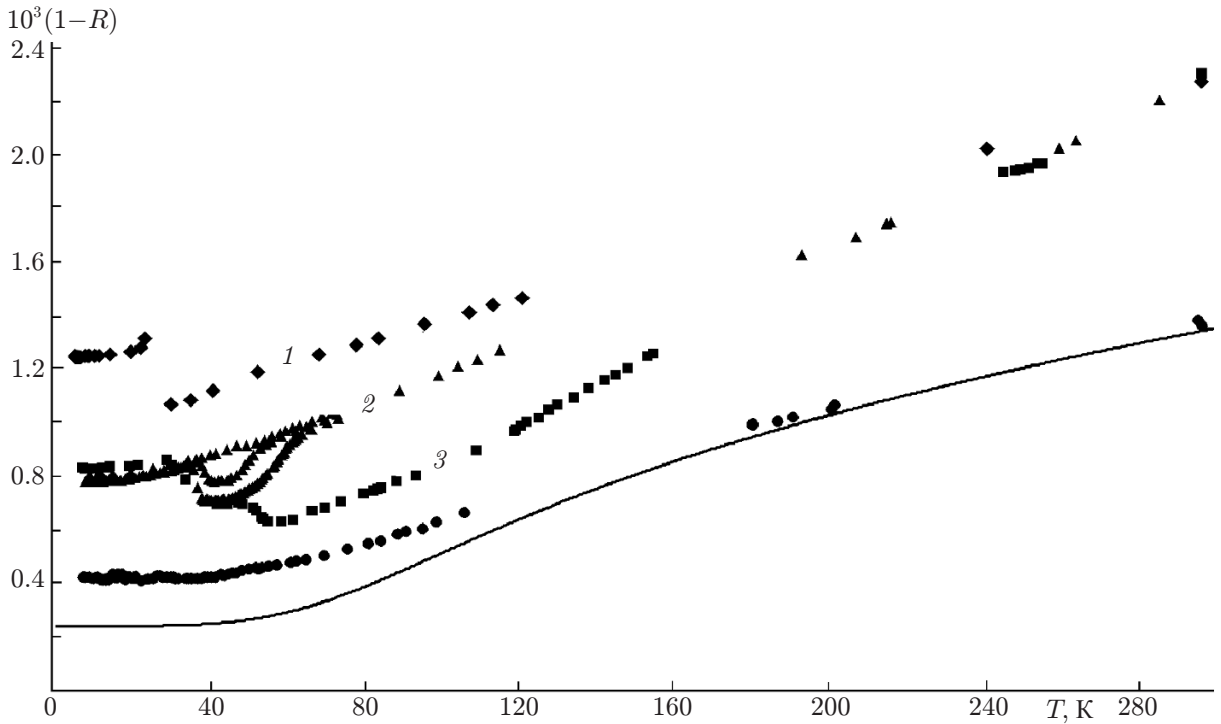


Fig. 5. Temperature dependences of the reflection loss for the film reflectors of the "Millimetron" space observatory (digits denote the numbers of the samples, see the text). Circles denote the reflection loss for the mirror of "thick" high-purity aluminum. The solid curve corresponds to the calculated dependence of the reflection loss for aluminum with allowance for the anomalous skin effect. The calculations and measurements were performed at a frequency of 150 GHz.

aluminum content was 99.99 wt%) and a data-sheet thickness of about $0.26 \mu\text{m}$, but were cut out of various places of a large sheet. Visually, sample 3 is almost opaque, whereas sample 2 is noticeably transparent for visible light. Three measurement cycles were carried out for sample 2 when it was cooled to 4 K. As was expected, the losses were smaller for the samples with larger aluminum thickness. However, even for samples 2 and 3 with thickness approximately equal to the skin depth, the losses are significantly higher

than those for a “thick” aluminum film.

In the range from 60 K to room temperature, the temperature dependences of losses are smooth and the measurement results coincide for each cycle. However, below 60 K a certain anomaly in the reflection loss is observed, and the result is not stable for each cycle even for the same sample. Since the losses in the samples after the cooling–heating cycle return to their initial values at a temperature of 300 K and a typical local extremum in the losses is observed for approximately the same temperature, it can be assumed that these phenomena are related to variations in the mechanical properties of aluminum films, which leads to the reflecting-surface distortion. (Note that the aluminum thickness is much smaller than the polyimide thickness and does not affect the mechanical properties of the reflector.) It is also possible that a certain rearrangement of the aluminum-layer internal structure occurs in the range 30–60 K. The obtained data do not allow us to draw unequivocal conclusions. Note that local extrema were not observed in the temperature dependence of the losses for bulk copper and aluminum mirrors.

The obtained measurements show that within the measurement error the reflection loss is constant and amounts to $2.3(2) \cdot 10^{-3}$ for all films in the frequency range 100–200 GHz at room temperature. This is indicative of the fact that the actual aluminum-layer thickness is smaller than that of the skin depth [22]. Such a mismatch of the aluminum-coating effective thickness corresponding to the experimental results can be attributed to the granular structure of the aluminum film, which is manufactured by vacuum deposition. However, since these discrepancies are not too large, the performed measurements allow one to formulate recommendations for the designers of the radiation screens of the “Millimetron” space observatory for optimizing the thickness of the screens operating at various temperatures, as well as the thickness and production process for the coatings of the cryogenic screen and the main mirror of the observatory.

4. CONCLUSIONS

We have developed a unique instrumental facility, which allows one to study dielectric characteristics of gases and condensed media, as well as surface reflectivity (reflection loss) in the frequency range 100–500 GHz and the pressure interval from 10^{-3} Torr to the atmospheric pressure in the temperature range 4–370 K.

The results presented in this work show the capabilities of this facility use for both fundamental studies and applied research.

The results of the studies indicate that the mirror cooling to below 60 K does not lead to any significant decrease in the reflection loss. However, since the reflector noise temperature is determined by the product of the reflection loss and the physical temperature of the reflector, deep cooling of all receiving reflectors is justified to reduce the noise temperature of the receiving channel.

The reflection losses for the film coatings whose data-sheet thickness is only slightly larger than the skin depth exceed the calculated values severalfold.

This work was partially supported the Ministry of Education and Science of the Russian Federation (project No. 11. G34.31.0029 within the framework of Order No. 220 of the Government of the Russian Federation) and the Russian Foundation for Basic Research (project Nos. 12–05–31170-mol_a, 12–05–00189, and 12–05–00309).

We express appreciation to A. I. Eliseev, A. E. Zargarov, D. V. Korotaev, and V. G. Perminov (Institute of Applied Physics of the Russian Academy of Sciences) for valuable recommendations and direct participation in the design and manufacturing of the facility elements, and to A. G. Litvak for support of the complex construction.

REFERENCES

1. Yu. A. Dryagin and V. V. Parshin, *Int. J. Infrared Millimeter Waves*, **13**, No. 7, 1023 (1992).
2. A. F. Krupnov, *Radiophys. Quantum Electron.*, **41**, No. 11, 923 (1998).
3. A. F. Krupnov, *Spectrochimica Acta A*, **52**, 967 (1996).
4. A. F. Krupnov, M. Yu. Tretyakov, V. V. Parshin, et al., *J. Mol. Spectrosc.*, **202**, No. 1, 107 (2000).
5. V. V. Parshin, M. Yu. Tretyakov, V. N. Shanin, and A. P. Shkaev, in: *22nd Russian Conf. on Radio Wave Propagation, Rostov-on-Don-Loo, September, 18–22, 2008*, p. 258.
6. M. Yu. Tretyakov, A. F. Krupnov, M. A. Koshelev, et al., *Rev. Sci. Instrum.*, **80**, No. 9, 093106 (2009).
7. V. N. Shanin, V. V. Dorovskikh, M. Yu. Tret'yakov, V. V. Parshin, and A. P. Shkaev, *Instrum. Exp. Tech.*, **46**, No. 6, 798 (2003).
8. V. V. Parshin, M. Yu. Tretyakov, M. A. Koshelev, and E. A. Serov, *IEEE Sensors J.*, **13**, No. 1, 18 (2013).
9. M. Yu. Tretyakov, M. A. Koshelev, I. N. Vilkov, et al., *J. Quant. Spectrosc. Rad. Trans.*, **114**, 109 (2013).
10. M. A. Koshelev, E. A. Serov, V. V. Parshin, and M. Yu. Tretyakov, *J. Quant. Spectrosc. Rad. Trans.*, **112**, 2704 (2011).
11. M. Yu. Tretyakov, V. V. Parshin, M. A. Koshelev, et al., *J. Mol. Spectrosc.*, **218**, 239 (2003).
12. D. S. Makarov, M. Yu. Tretyakov, and P. W. Rosenkranz, *J. Quant. Spectrosc. Rad. Trans.*, **112**, 1420 (2011).
13. M. Yu. Tretyakov, E. A. Serov, M. A. Koshelev, et al., *Phys. Rev. Lett.*, **110**, No. 9, 093001 (2013).
14. V. F. Vdovin, *Radiophys. Quantum Electron.*, **48**, Nos. 10–11, 779 (2005).
15. W. Wild, N. S. Kardashev, S. F. Likchachev, et. al., *Exp. Astron.*, **10**, DOI 10.1007/s1-686-008-9097-6 (2008).
16. V. V. Parshin, in: *Proc. the 6th Int. Conf. on Antenna Theory and Techniques (ICATT'07), Sevastopol, Ukraine, 2007*, p. 71.
17. V. V. Parshin, C. G. M. van't Klooster, and E. A. Serov, in: *Proc. the 30th ESA Antenna Workshop on Antennas for Earth Observation, Science, Telecommunication and Navigation Space Missions, Noordwijk, The Netherlands, May 27–30, 2008*, p. 353.
18. V. V. Parshin, E. A. Serov, C. G. M., van't Klooster, and P. Noschese, in: *Proc. the 5th ESA Workshop on Millimetre Wave Technology and Applications and the 31st ESA Antenna Workshop, The Netherlands, 2009*, p. 593..
19. R. B. Dingle, *Physica*, **19**, 311 (1953).
20. A. A. Abrikosov, *Fundamentals of the Theory of Metals*, North-Holland, New York (1988).
21. N. N. Prentslau, *Low Temp. Phys.*, **25**, No. 10, 782 (1999).
22. A. E. Kaplan, *Radiotekh. Électron.*, **9**, No. 10, 1781 (1964).